arXiv:2301.12183v1 [astro-ph.IM] 28 Jan 2023

White Paper for the 2024 Solar & Space Physics Decadal Survey

Radio Studies of the Middle Corona

Current State and New Prospects in the Next Decade

Principal Author:
Bin Chen[1] *New Jersey Institute of Technology*
Email: binchen@njit.edu; Phone: (973) 596-3565; Web: https://binchensun.org

Co-authors
Jason E. Kooi[2], David B. Wexler[3], Dale E. Gary[1], Sijie Yu[1], Surajit Mondal[1], Adam R. Kobelski[4], Daniel B. Seaton[5], Matthew J. West[5], Stephen M. White[6], Gregory D. Fleishman[1], Pascal Saint-Hilaire[7], Peijin Zhang[8], Chris R. Gilly[9], James P. Mason[10], Hamish Reid[11]

[1] New Jersey Institute of Technology; [2] Naval Research Laboratory; [3] University of Massachusetts, Lowell; [4] NASA Marshall Space Flight Center; [5] Southwest Research Institute; [6] Air Force Research Laboratory; [7] University of California, Berkeley; [8] Bulgaria Academy of Sciences, Bulgaria; [9] Laboratory for Atmospheric and Space Physics; [10] Johns Hopkins University Applied Physics Laboratory; [11] University College London

Co-Signers & Affiliations: see spreadsheet

Synopsis
The "middle corona," defined by West et al. (2022) as the region between ∼1.5–6 $R_\odot$, is a critical transition region that connects the highly structured lower corona to the outer corona where the magnetic field becomes predominantly radial. At radio wavelengths, remote-sensing of the middle corona falls in the meter–decameter wavelength range where a critical transition of radio emission mechanisms occurs. In addition, plasma properties of the middle corona can be probed by trans-coronal radio propagation methods including radio scintillation and Faraday rotation techniques. Together they offer a wealth of diagnostic tools for the middle corona, complementing current and planned missions at other wavelengths. These diagnostics include unique means for detecting and measuring the magnetic field and energetic electrons associated with coronal mass ejections, mapping coronal shocks and electron beam trajectories, as well as constraining the plasma density, magnetic field, and turbulence of the "young" solar wind. Following a brief overview of pertinent radio diagnostic methods, this white paper will discuss the current state of radio studies on the middle corona, challenges to obtaining a more comprehensive picture, and recommend an outlook in the next decade. Our specific recommendations for advancing the middle coronal sciences from the radio perspective are:

- Prioritizing solar-dedicated radio facilities in the ∼0.1–1 GHz range with broadband, high-dynamic-range imaging spectropolarimetry capabilities.
- Developing facilities and techniques to perform multi-perspective, multiple lines-of-sight trans-coronal radio Faraday Rotation measurements.

1 Introduction

The middle corona, defined by West et al. as the region from $\sim$1.5–6 $R_\odot$, features a key transition between the inner and the outer solar corona where, in general, the magnetic field of the background corona changes from predominantly closed to radial, and the plasma β goes from low to high values. Consequently, this region is highly dynamic in nature and hosts a plethora of key physical processes. While the importance of this region has long been recognized, the middle corona remains poorly understood, due primarily to the lack of observations. The importance of understanding the middle corona and strategic recommendations based on integrated multi-wavelength, multi-messenger observational approaches are discussed in the white paper by Seaton et al. In this white paper, we focus on the specific aspects that can be addressed by radio observing techniques.

There exist a number of mechanisms relevant to radio emissions from the solar corona, which include gyroresonance (thermal electrons gyrating in the coronal magnetic field), gyrosynchrotron (nonthermal electrons gyrating in the coronal magnetic field), bremsstrahlung (or free-free; electrons interacting with ions), as well as a variety of coherent emissions such as plasma radiation (e.g. the nonlinear growth of Langmuir waves) and electron cyclotron masers (i.e. the nonlinear growth of plasma waves at harmonics of the electron cyclotron frequency). These emission mechanisms co-exist, but because the physical parameters differ in various coronal locations/conditions, the importance of each emission mechanism also varies. In particular, the plasma density n_e and magnetic field B vary dynamically throughout the corona, and hence the corresponding plasma frequency ν_p and gyrofrequency $\nu_{\rm B}$. As a result, the dominant radio emission mechanism varies over the corona and can change due to local conditions.

From the perspective of radio observers, the middle corona includes the coronal heights where the mechanism producing solar radio bursts undergoes a key transition from incoherent radio emission to coherent radio emission. Figure 1 (adapted from Gary & Hurford 2004) shows the variation of plasma frequency (ν_p; thick black curve), gyrofrequency ($\nu_{\rm B}$; thin black curve), and the frequency of the free-free opacity $\sim$1 ($\nu_\tau = 1$) layer as a function of coronal height under typical quiescent coronal conditions.

The transition region and the innermost inner corona ($\lesssim$ 1.1 $R_\odot$ from the center of the Sun) are dominated by incoherent gyromagnetic emission and free-free emission. At around 1.5 $R_\odot$, the plasma frequency ν_p layer takes over and becomes higher (closer to the observer) than both the $\nu_\tau = 1$ curve and the curves of $\nu_{\rm B}$ and its harmonics. Such a transition has a profound implication for radio observations: the quiescent free-free radio corona is no longer playing a dominant role due to the strong refraction near the plasma frequency. Meanwhile, bright coherent radio bursts, due to plasma radiation occurring near $\nu_{\rm p}$ and its second harmonic (or electron cyclotron maser emission at low harmonics of $\nu_{\rm B}$ if the magnetic field is strong — see discussion in a white paper by Yu et al.), start to be important among the observed radio phenomena. Of course, even in the region where the coherent plasma radiation dominates, incoherent radio emission from coronal transients can still be observed, providing crucial diagnostics for these transients. Outstanding examples may include measuring the magnetic field and nonthermal electrons trapped in coronal mass ejection (CMEs) cavities or accelerated by CME-driven shocks (see another white paper by Chen et al. 2022). Therefore, at radio wavelengths, a broad frequency range of $<$10 MHz to $\sim$1 GHz is relevant to the highly dynamic and structured middle corona (light pink box in Figure 1). It is worth emphasizing that the magnetic field and non-thermal electron distribution diagnostics in

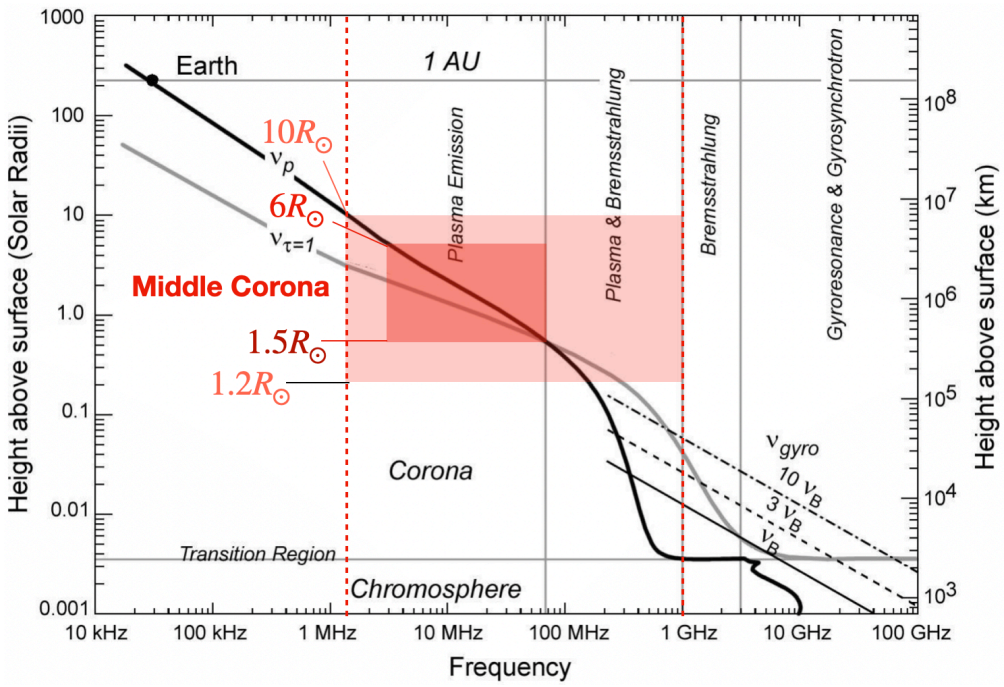


Figure 1: Characteristic radio frequencies in the solar atmosphere. The middle corona includes a critical region where the transition of radio emission mechanisms occurs. The dark pink box marks the nominal range of the middle corona ($\sim$1.5–6 $R_\odot$) and the light pink box marks an extended range taking into account the highly structured and dynamic nature of the corona. The corresponding frequencies that are relevant to radio observations of the middle corona range from $<$10 MHz to $\sim$1 GHz. (Adapted from Gary & Hurford 2004 who describe the sources for the temperature, density and magnetic field values used in this plot.)

the middle corona are unique to the radio techniques, since the relatively low density in the middle corona limits emission due to nonthermal particles at other wavelengths (such as X-rays).

Additionally, when radio waves from known, point-like external sources (either natural celestial sources such as quasars/pulsars or spacecraft transmitters) traverse the corona, their propagation and polarization signatures are modulated. The observed temporal and spectral variations provide other means for studying the middle corona. The observed radio signatures can be used to probe the structure and dynamics of the middle corona, including density inhomogeneities, solar wind speed, and coronal magnetic field and its fluctuations. Importantly, these trans-coronal radio sensing methods are applicable in all solar activity states and do not rely on observations of specific episodic outburst phenomena, although spatially resolved diagnostics require measurements along different lines of sight (see white papers by Kooi et al. 2022a and Kooi et al. 2022b).

2 Radio Phenomena and Diagnostics in the Middle Corona

By virtue of the transitional nature of the radio emission mechanisms in the middle corona, radio observations offer a rich variety of diagnostics for both the background coronal plasma and solar

wind, as well as transient phenomena such as CMEs. In the following, we provide a brief overview on various radio phenomena pertinent to the middle corona and the associated diagnostic methods.

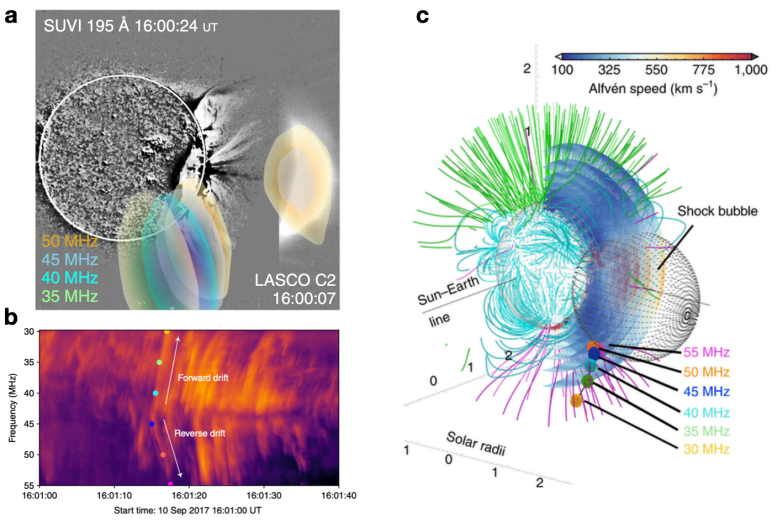


Figure 2: LOFAR observations of a decametric type II radio burst event associated with a large-scale coronal shock. a) LOFAR imaging of the burst at the nose and flank of the CME-driven shock. b) "Herringbone" fine structures associated with the type II burst, interpreted as the signature of fast electron beams escaping from the shock front. c) 3D model of the magnetic field and the shock geometry. (Adapted from Morosan et al. 2019.)

Type II Bursts and Coronal Shocks

Type II radio bursts are seen from metric to kilometric wavelengths (a few times 100 MHz to 10s of kHz) and are notable for their relatively slow drift to lower frequencies compared to type III radio bursts (see below). They are due to coherent plasma radiation of energetic electrons accelerated at or near the shock front propagating outward at super-Alfvénic speeds. Therefore, they bear important diagnostics for both the shock parameters and shock-accelerated electrons. The band-splitting features in type II radio bursts can be used to derive the magnetic Mach number of the shock front Vršnak et al. (2004). Figure 2 shows an example of a type II burst that displays a "herringbone" feature in the time-frequency domain. This feature is interpreted as the signature of fast electron beams escaping from the shock front. Recently, thanks to the imaging spectroscopy capability provided by instruments such as LOFAR, new insights have been obtained into their source region at the CME-driven shock (panel (c) of Fig. 2).

Type III Bursts and Electron Beams

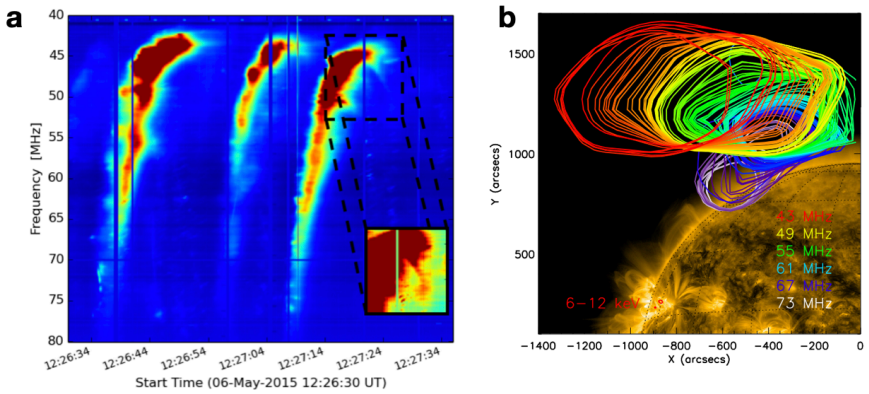


Figure 3: LOFAR observations of a type III radio burst event in the middle corona. Multi-frequency images on the right show the trajectory of a type-III-burst-emitting electron beam propagating from low to middle corona. (Adapted from Reid & Kontar 2017.)

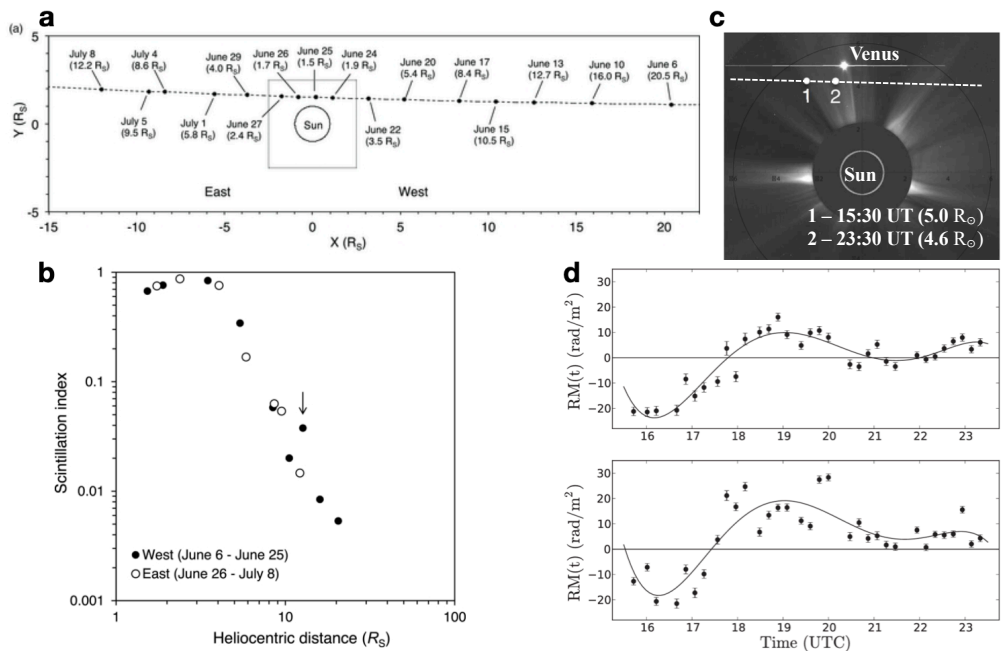


Figure 4: Diagnostics of the middle corona via radio propagation methods. (a) and (b) Radio scintillation index, which represents the magnitude of intensity fluctuations, as a function of heliocentric distance (Imamura et al. 2014). (c) and (d) Faraday rotation provides information on the plasma density and magnetic field component along the line of sight. Differences between measurements along 2+ lines of sight can be used to probe coronal electric currents (Kooi et al. 2014).

Type III radio bursts are produced by fast electron beams ($\sim$0.1–0.5c) escaping along open magnetic field lines (see, e.g., Reid & Ratcliffe 2014; Reid 2020 for recent reviews). Observations of type III bursts span an extremely wide frequency range from >GHz to kHz and exhibit a much greater frequency drift than that of type II bursts. In the middle corona, these bursts are predominantly associated with open field lines. With imaging spectroscopy provided by general-purpose facilities such as LOFAR and MWA, new advances have been made in tracing the trajectories of the electron beams (Fig. 3) which, in turn, outline the electron-beam-conducting magnetic field lines threading the middle corona (e.g. McCauley et al. 2017; Mann et al. 2018). The technique of imaging spectroscopy also has the potential to pinpoint the elusive electron acceleration site(s) (Reid et al. 2011), akin to that achieved in the lower corona with the Jansky VLA (Chen et al. 2018). The emission frequencies and fine structures in the dynamic spectra have been used to derive the coronal density variation in height and properties of the coronal turbulence (Kontar et al. 2017; McCauley et al. 2018; Mann et al. 2018; Reid & Kontar 2021).

Type IV Bursts and Trapped Electrons

Type IV radio bursts are broadband bursts characterized by their slow- or non-drifting appearance in the dynamic spectrum. Typically observed after the flare peak, they are thought to be produced by nonthermal electrons trapped in closed coronal structures. Depending on the underlying emission mechanism (which can be coherent or incoherent), type IV bursts can, on one hand, outline the closed magnetic structure of interest, and on the other hand, provide diagnostics of the source region (see, e.g., review by Carley et al. 2020, and references therein). Type IV radio bursts have been generally sub-categorized into stationary and moving type IV bursts. The latter, by virtual of

their close association with CMEs, are of particular interest.

Radio CMEs
Faint radio emissions that closely resemble their white light CME counterparts are dubbed "radio" CMEs because of their similar appearance (see recent review by Vourlidas et al. 2020). The emission mechanism is believed to be synchrotron emission, which occurs at large harmonics of the electron gyrofrequency and is thus well above the local plasma frequency, thereby being less affected by the scattering effects (compared to, e.g., the coherent bursts discussed above). Thanks to their incoherent nature, when imaged at multiple frequencies, radio CMEs can be used to map the coronal magnetic field strength (and, possibly, the plane-of-sky direction if polarimetry is available) and non-thermal electron distribution associated with the CMEs (see, e.g. Bastian et al. 2001). For more details on radio diagnostics of CMEs and their progenitors, please refer to another white paper by Chen et al. (2022).

Propagation Effects
The propagation effects of radio waves provide another means for studying the middle corona. For example, signal broadening and scintillation provide information on the density inhomogeneities in the turbulent coronal plasma (Rickett 1990). Analysis of radio scintillation and frequency fluctuations (Figure 4(a) and (b)) can provide estimates of solar wind speed (Imamura et al. 2014; Wexler et al. 2019, 2020). In addition, modulations of the signal polarization due to Faraday rotation (Figure 4(c) and (d)) and coronal birefringence can be used to constrain the coronal magnetic field and its fluctuations (see, e.g. Wexler et al. 2017, 2021; Kooi et al. 2021, 2022c; Kobelski et al. 2022, and references therein).

3 Current Radio Instrumentation

Observing the middle corona at radio wavelengths requires accessing a wide frequency range from $<$10 MHz to $\sim$1 GHz (c.f. Figure 1). The $>$20 MHz range is generally accessible from the ground, but the lowest frequencies can only be observed from space due to the ionospheric cutoff. Currently, multiple ground-based instruments are available to observe the frequency range relevant to the middle corona. In space, new missions, such as the Sun Radio Interferometer Space Experiment (SunRISE; Kasper et al. 2022), are being commissioned to locate radio bursts in the upper portion of the middle corona. Table 1 summarizes the currently operating and upcoming radio facilities that provide imaging capabilities in the frequency range relevant to middle corona studies. This list does not include the large number of radio instruments that provide total-power (full-Sun integrated) dynamic spectral measurements such as the US Air Force's Radio Solar Telescope Network (RSTN) and the e-Callisto network (Benz et al. 2009).

Over the past decade, new advances have been made with radio facilities equipped with *broadband dynamic imaging spectroscopy*. This exciting new technique allows simultaneous imaging and spectroscopy to be performed over a broad frequency range and at a high time cadence. In other words, a detailed spectrum can be derived from *each pixel* in the radio image for spectral analysis. First realized by the Karl G. Jansky Very Large Array (JVLA) at the decimetric wavelengths (Chen et al. 2013) and followed by the commissioning of LOFAR, MWA, EOVSA, and OVRO-LWA, this technique is just beginning to reach the full potential of radio studies using the rich diagnostics tools available (e.g. Carley et al. 2020). Figs. 2 and 3 show outstanding examples from LOFAR, which is a general-purpose radio facility (i.e., proposal-driven).

Facility	Frequency Range	Elements	Max Baseline	Angular Resolution	Mid-day UT	Solar Dedicated?
MUSER-I[a] (China)	400–2000 MHz	40	∼3 km	∼1′ at 400 MHz	04 UT	Yes
Nancay[b] (France)	150–450 MHz	47	∼3 km	∼1′ at 400 MHz	12 UT	Yes
GRAPH[c] (India)	40–150 MHz	32	1.3 km (EW) 0.44 km (NS)	5–8′ at 150 MHz	07 UT	Yes
OVRO-LWA[d] (USA)	20–88 MHz	48	2.6 km	∼5′ at 80 MHz	20 UT	Yes
uGMRT[e] (India)	120–1450 MHz	30	25 km	4″ at 650 MHz[j]	07 UT	No
JVLA P Band[f] (USA)	230–470 MHz	27	3.4 km (C config.)	$\lesssim$1′ at 400 MHz	19 UT	No
MWA (Australia)[g]	80–300 MHz	128	∼5 km	1.3′ at 150 MHz	04 UT	No
LOFAR (Netherlands)	20–80 MHz (LBA)[h] 120–180 MHz (HBA)[i]	52	>48 km	<16″ at 80 MHz[j]	13 UT	No

[a] Yan et al. (2021). [b] Kerdraon & Delouis (1997). [c] Ramesh et al. (1998). [d] Chhabra et al. (2021). [e] Gupta et al. (2017). [f] See JVLA's 2023A performance. [g] Beardsley et al. (2019). [h] Zhang et al. (2022). [i] Liu et al. (2022). [j] Note the values quoted here are the *theoretical* resolution ($\lambda/d_{\max}$). The actual resolution is limited by coronal scattering.

Table 1: Current radio facilities that provide radio imaging capabilities relevant to middle corona studies.

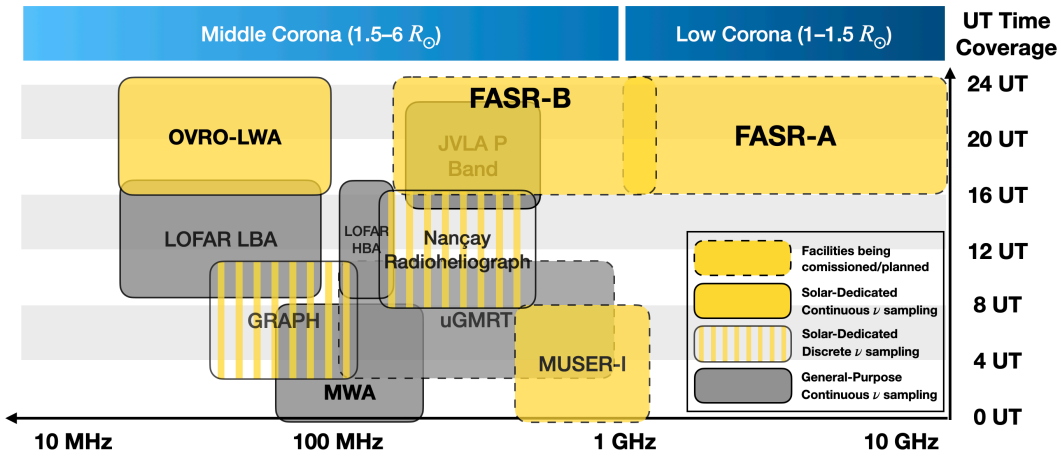


Figure 5: Frequency and UT time coverage of radio imaging facilities listed in Table 1. Filled yellow boxes indicated solar-dedicated instruments with continuous frequency sampling. FASR-B will fill the gap between 0.2–2 GHz in the UT range of ∼16–24 UT, by providing radio observations with superior broadband imaging spectropolarimetry.

4 Future Prospects and Recommendations

For radio imaging observations of the middle corona, while multiple facilities are available around the globe, currently **there is no solar-dedicated radio instrument available to provide true broadband dynamic imaging spectroscopy in the ∼0.1–1 GHz spectral range** (see Fig. 5).

Such a missing capability is critical to producing observations in support of key open questions about the middle corona (see recommendations in Seaton et al. 2022). As discussed in Section 2, these observations include but are not limited to tracing coronal shocks and shock-accelerated particles, mapping trajectories of fast electron beams from the reconnection site(s), understanding CME initiation and acceleration, understanding CME-accelerated electrons, and providing unique measurements of the evolving magnetic field of CMEs in the middle corona.

To exploit the unique diagnostics of radio observations to the background corona and transient events in the middle corona, the following instrumental requirements must be fulfilled with multiple ground-based and space-borne facilities:

- Frequency coverage: continuous coverage from $\sim$1 MHz to $\sim$1 GHz to enable access to the entire middle corona. The $\sim$20 MHz–1 GHz range can be done from the ground, while the $\lesssim$20 MHz range needs to be performed from space due to the ionospheric cutoff.
- High-dynamic-range imaging: a dynamic range of $>$1000:1 is needed at each frequency to detect and map faint and diffuse structures such as radio CMEs. This requirement necessitates a ground-based radio facility with a large number of antenna elements (of order 100).
- Adequate angular resolution: scattering in the corona limits the usable angular resolution (Bastian 1994; Kontar et al. 2019). Resolving structures down to the scattering limit in $\sim$20 MHz–1 GHz translates to an interferometer with a footprint of 3–4 km, which has a resolution of $\sim 1'$ at 400 MHz. This is sufficient to resolve most features of interest in the middle corona including streamers and CMEs.
- Adequate spectral resolution: a spectral resolution of $\Delta\nu/\nu \approx 1\%$ is needed to observe coherent radio bursts, although an even higher resolution may be necessary to resolve fine structures such as Type III striae (e.g., Reid & Kontar 2021).
- High time resolution: to resolve fast temporal structures of coherent bursts, a time resolution of order 0.1 s is needed. At the high-frequency end ($\sim$1 GHz), a higher time resolution of order 0.01 s is desired (e.g., Chen et al. 2018).
- Dual-polarization performance: Measurements of the total intensity are required as are those of the Stokes V parameter, which contains quantitative information about the magnetic field in, e.g., CMEs.

These requirements for advancing radio studies of the middle corona science from the ground already comprise one of the core objectives of the *Frequency Agile Solar Radiotelescope* (FASR) concept, which is envisioned to provide high resolution, high dynamic range, and high fidelity dynamic imaging spectroscopy over a wide frequency range from 0.2–20 GHz. For more details about FASR, we direct the readers to the white paper by Gary et al. (2022).

For new frontiers in trans-coronal radio techniques, particularly in extracting the line-of-sight (LOS) magnetic field information of the middle corona in a wide range of helio-altitudes and longitudes, multi-perspective, multiple LOS observations are required. This objective could be achieved by having a large set of small spacecraft fleet transmitting radio signals through the corona at various low impact parameters towards terrestrial radio telescope receivers. In addition, new developments for the Faraday Rotation (FR) tomography method by utilizing 100s of natural background sources can lead to the construction of 2D FR sky maps. A spacecraft fleet concept and new techniques on this front are discussed in white papers by Kooi et al. (2022a) and Kooi et al. (2022b).

References

Bastian, T. S. 1994, *Angular Scattering of Solar Radio Emission by Coronal Turbulence*, ApJ, 426, 774, 10.1086/174114

Bastian, T. S., Pick, M., Kerdraon, A., et al. 2001, *The Coronal Mass Ejection of 1998 April 20: Direct Imaging at Radio Wavelengths*, ApJ, 558, L65, 10.1086/323421

Beardsley, A. P., Johnston-Hollitt, M., Trott, C. M., et al. 2019, *Science with the Murchison Wide-field Array: Phase I results and Phase II opportunities*, PASA, 36, e050, 10.1017/pasa.2019.41

Benz, A. O., Monstein, C., Meyer, H., et al. 2009, *A World-Wide Net of Solar Radio Spectrometers: e-CALLISTO*, Earth Moon and Planets, 104, 277, 10.1007/s11038-008-9267-6

Carley, E. P., Vilmer, N., & Vourlidas, A. 2020, *Radio observations of coronal mass ejection initiation and development in the low solar corona*, Frontiers in Astronomy and Space Sciences, 7, 79, 10.3389/fspas.2020.551558

Carley, E. P., Baldovin, C., Benthem, P., et al. 2020, *Radio observatories and instrumentation used in space weather science and operations*, Journal of Space Weather and Space Climate, 10, 7, 10/gh88nh

Chen, B., Bastian, T. S., White, S. M., et al. 2013, *Tracing Electron Beams in the Sun's Corona with Radio Dynamic Imaging Spectroscopy*, ApJ, 763, L21, 10.1088/2041-8205/763/1/L21

Chen, B., Yu, S., Battaglia, M., et al. 2018, *Magnetic Reconnection Null Points as the Origin of Semirelativistic Electron Beams in a Solar Jet*, ApJ, 866, 62, 10.3847/1538-4357/aadb89

Chen, B., Fan, Y., Gibson, S., et al. 2022, *Radio Diagnostics of CMEs and CME Progenitors*, White Paper Submitted to the Decadal Survey for Solar and Space Physics

Chhabra, S., Gary, D. E., Hallinan, G., et al. 2021, *Imaging Spectroscopy of CME-associated Solar Radio Bursts Using OVRO-LWA*, ApJ, 906, 132, 10.3847/1538-4357/abc94b

Gary, D., Chen, B., Fleishman, G., et al. 2022, *Frequency Agile Solar Radiotelescope: A Next-Generation Radio Telescope for Solar Physics and Space Weather*, White Paper Submitted to the Decadal Survey for Solar and Space Physics

Gary, D. E., & Hurford, G. J. 2004, in Astrophysics and Space Science Library, Vol. 314, Astrophysics and Space Science Library, ed. D. E. Gary & C. U. Keller, 71, 10.1007/1-4020-2814-8_4

Gupta, Y., Ajithkumar, B., Kale, H. S., et al. 2017, *The upgraded GMRT: opening new windows on the radio Universe*, Current Science, 113, 707, 10.18520/cs/v113/i04/707-714

Imamura, T., Tokumaru, M., Isobe, H., et al. 2014, *Outflow Structure of the Quiet Sun Corona Probed by Spacecraft Radio Scintillations in Strong Scattering*, ApJ, 788, 117, 10.1088/0004-637X/788/2/117

Kasper, J., Lazio, T. J. W., Romero-Wolf, A., et al. 2022, in 2022 IEEE Aerospace Conference (AERO), 1–8, 10.1109/AERO53065.2022.9843607

Kerdraon, A., & Delouis, J.-M. 1997, in Coronal Physics from Radio and Space Observations, ed. G. Trottet, Vol. 483, 192, 10.1007/BFb0106458

Kobelski, A., Mondal, S., Chen, B., et al. 2022, *Radio Observations of the Quiet Chromosphere and Corona*, White Paper Submitted to the Decadal Survey for Solar and Space Physics

Kontar, E. P., Yu, S., Kuznetsov, A. A., et al. 2017, *Imaging spectroscopy of solar radio burst fine structures*, Nature Communications, 8, 1515, 10.1038/s41467-017-01307-8

Kontar, E. P., Chen, X., Chrysaphi, N., et al. 2019, *Anisotropic Radio-wave Scattering and the Interpretation of Solar Radio Emission Observations*, ApJ, 884, 122, 10.3847/1538-4357/ab40bb

Kooi, J., Wexler, D., Jensen, E., et al. 2022a, *How to Advance Studies of Coronal Faraday Rotation*, White Paper Submitted to the Decadal Survey for Solar and Space Physics

—. 2022b, *Progressing Towards Faraday Rotation Tomography of the Solar Wind*, White Paper Submitted to the Decadal Survey for Solar and Space Physics

Kooi, J. E., Ascione, M. L., Reyes-Rosa, L. V., et al. 2021, *VLA Measurements of Faraday Rotation Through a Coronal Mass Ejection Using Multiple Lines of Sight*, Sol. Phys., 296, 11, 10.1007/s11207-020-01755-4

Kooi, J. E., Fischer, P. D., Buffo, J. J., et al. 2014, *Measurements of Coronal Faraday Rotation at 4.6 $R_\odot$*, ApJ, 784, 68, 10.1088/0004-637X/784/1/68

Kooi, J. E., Wexler, D. B., Jensen, E. A., et al. 2022c, *Modern Faraday Rotation Studies to Probe the Solar Wind*, Frontiers in Astronomy and Space Sciences, 9, 841866, 10.3389/fspas.2022.841866

Liu, H., Zucca, P., Cho, K.-S., et al. 2022, *Interferometric imaging, and beam-formed study of a moving Type IV Radio burst with LOFAR*, arXiv preprint arXiv: Arxiv-2208.13670, arXiv.2208.13670

Mann, G., Breitling, F., Vocks, C., et al. 2018, *Tracking of an electron beam through the solar corona with LOFAR*, A&A, 611, A57, 10.1051/0004-6361/201629017

McCauley, P. I., Cairns, I. H., & Morgan, J. 2018, *Densities Probed by Coronal Type III Radio Burst Imaging*, Sol. Phys., 293, 132, 10.1007/s11207-018-1353-y

McCauley, P. I., Cairns, I. H., Morgan, J., et al. 2017, *Type III Solar Radio Burst Source Region Splitting due to a Quasi-separatrix Layer*, ApJ, 851, 151, 10.3847/1538-4357/aa9cee

Morosan, D. E., Carley, E. P., Hayes, L. A., et al. 2019, *Multiple regions of shock-accelerated particles during a solar coronal mass ejection*, Nature Astronomy, 3, 452, 10.1038/s41550-019-0689-z

Ramesh, R., Subramanian, K. R., Sundararajan, M. S., et al. 1998, *The Gauribidanur Radioheliograph*, Sol. Phys., 181, 439, 10.1023/A:1005075003370

Reid, H. A. S. 2020, *A review of recent type III imaging spectroscopy*, Frontiers in Astronomy and Space Sciences, 7, 56, 10.3389/fspas.2020.00056

Reid, H. A. S., & Kontar, E. P. 2017, *Imaging spectroscopy of type U and J solar radio bursts with LOFAR*, A&A, 606, A141, 10.1051/0004-6361/201730701

—. 2021, *Fine structure of type III solar radio bursts from Langmuir wave motion in turbulent plasma*, Nature Astronomy, 5, 796, 10.1038/s41550-021-01370-8

Reid, H. A. S., & Ratcliffe, H. 2014, *A Review of Solar Type III Radio Bursts*, Research in Astronomy and Astrophysics, 14, 773, 10.1088/1674-4527/14/7/003

Reid, H. A. S., Vilmer, N., & Kontar, E. P. 2011, *Characteristics of the flare acceleration region derived from simultaneous hard X-ray and radio observations*, A&A, 529, A66, 10.1051/0004-6361/201016181

Rickett, B. J. 1990, *Radio propagation through the turbulent interstellar plasma.*, Annual Rev. Astron. Astrophys., 28, 561, 10.1146/annurev.aa.28.090190.003021

Seaton, D. B., West, M. J., Wexler, D. B., et al. 2022, *A Strategy to Close Key Questions about the Middle Solar Corona During this Decade*, White Paper Submitted to the Decadal Survey for Solar and Space Physics

Vourlidas, A., Carley, E. P., & Vilmer, N. 2020, *Radio Observations of Coronal Mass Ejections: Space Weather Aspects*, Frontiers in Astronomy and Space Sciences, 7, 43, 10.3389/fspas.2020.00043

Vršnak, B., Magdalenić, J., & Zlobec, P. 2004, *Band-splitting of coronal and interplanetary type II bursts-III. Physical conditions in the upper corona and interplanetary space*, Astronomy & Astrophysics, 413, 753

West, M. J., Seaton, D. B., Wexler, D. B., et al. 2022, *Defining the Middle Corona*, arXiv e-prints, arXiv:2208.04485. https://arxiv.org/abs/2208.04485

Wexler, D., Imamura, T., Efimov, A., et al. 2020, *Coronal Electron Density Fluctuations Inferred from Akatsuki Spacecraft Radio Observations*, Sol. Phys., 295, 111, 10.1007/s11207-020-01677-1

Wexler, D. B., Hollweg, J. V., Efimov, A. I., et al. 2019, *Spacecraft Radio Frequency Fluctuations in the Solar Corona: A MESSENGER-HELIOS Composite Study*, ApJ, 871, 202, 10.3847/1538-4357/aaf6a8

Wexler, D. B., Jensen, E. A., & Heiles, C. 2021, *Middle Corona Magnetic Field Strength Determined by Spacecraft Radio Faraday Rotation*, Research Notes of the American Astronomical Society, 5, 165, 10.3847/2515-5172/ac1521

Wexler, D. B., Jensen, E. A., Hollweg, J. V., et al. 2017, *Faraday rotation fluctuations of MESSENGER radio signals through the equatorial lower corona near solar minimum*, Space Weather, 15, 310, 10.1002/2016SW001558

Yan, Y., Chen, Z., Wang, W., et al. 2021, *Mingantu Spectral Radioheliograph for Solar and Space Weather Studies*, Frontiers in Astronomy and Space Sciences, 8, 20, 10.3389/fspas.2021.584043

Yu, S., Chen, B., Gary, D. E., et al. 2022, *Coherent ECM emission and solar-stellar connection*, White Paper Submitted to the Decadal Survey for Solar and Space Physics

Zhang, P., Zucca, P., Kozarev, K., et al. 2022, *Imaging of the Quiet Sun in the Frequency Range of 20-80 MHz*, ApJ, 932, 17, 10.3847/1538-4357/ac6b37